

Constraints on a k-dependent bias from galaxy clustering

E Menegoni¹

¹ CNRS, Laboratoire Univers et Theories (LUTh), UMR 8102 CNRS, Observatoire de Paris, Université Paris Diderot; 5 Place Jules Janssen, 92190 Meudon, France

E-mail: eloisa.menegoni@gmail.com

Abstract. We forecast the future constraints on scale-dependent parametrizations of galaxy bias and their impact on the estimate of cosmological parameters from the power spectrum of galaxies: in our approach we perform a Fisher matrix analysis with two different parametrizations of scale-dependent bias. The two main results obtained from the analysis are: first, allowing for a scale-dependent bias does not significantly increase the errors on the other cosmological parameters apart from the *rms* amplitude of density fluctuations, σ_8 , and the growth index γ , whose uncertainties increase by a factor up to two, depending on the bias model adopted. Second, we find that the accuracy in the linear bias parameter b_0 can be estimated to within 1-2% at various redshifts regardless of the fiducial model. The non-linear bias parameters have significantly large errors that depend on the model adopted.

1. Introduction

In the next future large experiments like DESI [1] and Euclid [2] will use galaxy clustering to simultaneously obtain information on the geometry of the Universe and the growth rate of density fluctuations by measuring the galaxy power spectrum. Since one typically observes the spatial fluctuation in the galaxy distribution, not in the mass, some independent phenomenological or theoretical insight of the mapping from one to the other is mandatory. This mapping, which is commonly referred to as *galaxy bias*, parametrises our ignorance on the physics of galaxy formation and evolution and represents perhaps the most serious source of uncertainties in the study of the large scale structure of the Universe [3].

It was shown in [4] that future galaxy redshift surveys contain enough information to break the degeneracy between the galaxy bias, the clustering amplitude and the growth factor, effectively allowing to estimate galaxy bias from the data themselves. We forecast the errors on cosmological parameters and galaxy bias parameters and we assess the robustness of our predictions against the choice of the bias and the fiducial model (for more details see [5]). We consider two different parametrizations for the scale-dependent bias: a simple power-law model and the polynomial model proposed by [6]. Both provide a reasonable good fit to mock galaxies similar to those that will be targeted by Euclid [7]. As dataset we assume a wide spectroscopic galaxy redshift survey spanning a large redshift range and consider, as a reference case, the upcoming Euclid survey [8].



2. Theoretical Setup

Following [9] we model the observed galaxy power spectrum, P_{obs} at the generic redshift z as:

$$P_{obs}(z, k) = G^2(z) b^2(k, z) \left(1 + \frac{f(z)}{b(z, k)} \mu^2\right)^2 \frac{D_{Af}^2(z) H(z)}{D_A^2(z) H_r(z)} P_{0r}(k) + P_{shot}(z) \quad (1)$$

where D_A is the angular-diameter distance, $H(z)$ is the so called expansion history, i.e. the Hubble constant at redshift z , $G(z)$ is the linear growth function normalized to unity at $z = 0$, $f(z) = d \log G / d \log a$ is the growth rate, $b(z, k)$ is the scale-dependent bias, $P_0(k)$ is the matter power spectrum at the present epoch, μ is the cosine angle between the wavenumber vector \vec{k} and the line of sight direction, P_{shot} is the Poisson shot noise contribution to the power spectrum and the subscript r identifies the fiducial model, this one is the case of scale-independent bias ($b_0 = 1$ and $n = 0$). We parametrize the growth rate as $f = \Omega_m^\gamma$ with a constant growth index γ .

We perform the forecast using the Fisher matrix information method, we approximate the likelihood as a Gaussian in the parameters around a particular fiducial model, i.e. a value of the parameters that is assumed to approximate the 2-point clustering properties of galaxies in the real Universe. We set $h_0 = 0.7$, $\Omega_{m0} = 0.25$; $\Omega_{b0} = 0.0445$; $\Omega_{k0} = 0$; the primordial slope $n_s = 1$; and the dark energy equation of state $w_0 = -0.95$. Finally, we set $\gamma = 0.545$ and rms density fluctuation at $8 h^{-1}$ Mpc $\sigma_8 = 0.8$ (for more technical details see [5]).

Assuming that the fluctuation Fourier modes are Gaussian variates, the Fisher matrix at each redshift shell is [10, 11]

$$F_{ij} = 2\pi \int_{k_{min}}^{k_{max}} \frac{\partial \log P(k_n)}{\partial \theta_i} \frac{\partial \log P(k_n)}{\partial \theta_j} \cdot V_{eff} \cdot \frac{k^2}{8\pi^3} \cdot dk \quad (2)$$

where the derivatives are evaluated at the parameter values of the fiducial model. Here, the maximum frequency $k_{max}(z)$ is set by the scale at which fluctuations grow nonlinearly while $k_{min}(z)$ by the largest scale that can be observed in the given redshift shell. We set a hard small scale cut-off $k_{max} = 0.5 h^{-1}$ Mpc at all redshifts which, together with the damping terms $P = P_{obs} e^{-k^2 \mu^2 \sigma_r^2}$ and $\exp \left\{ -k^2 \left[\frac{(1-\mu^2)\Sigma_\perp^2}{2} + \frac{\mu^2 \Sigma_\parallel^2}{2} \right] \right\}$ account for non linearities [5]. On large scale we set $k_{min} = 0.001 h^{-1}$ Mpc. V_{eff} indicates the effective volume of the survey defined as:

$$V_{eff} \equiv \int \left[\frac{n(\vec{r}) P(k, \mu)}{n(\vec{r}) P(k, \mu) + 1} \right]^2 d\vec{r} = \left[\frac{n P(k, \mu)}{n P(k, \mu) + 1} \right]^2 V_{survey} \quad (3)$$

where $n = n(z)$ is the galaxy density at redshift z . The second equality in Equation (3) holds if the co-moving number density is constant within the volume considered. This assumption, which we adopt in our analysis, is approximately true in a sufficiently narrow range of redshifts. For this reason, we perform the Fisher matrix analysis in different, non-overlapping redshift bins, together with their mean galaxy number density. The redshift range, the size of the bin and the number density of objects roughly match the analogous quantities that are expected in the Euclid spectroscopic survey (see [5]).

2.1. Analytic models for scale-dependent bias

Our goal is to assess the impact of a scale-dependent galaxy bias $b(z, k)$ in the analysis of future galaxy surveys [10]: for this purpose we have decided to adopt two rather simple models, the Power Law and the Q-Model. The reason for choosing these models are found in their simple

Table 1. Bias parameters for the fiducial models considered in this work (see [5]).

	$n = 0$	FM1-PL				FM1-Q		
		$n = 1$	$n = 2$	$n = 1$	$n = 2$	b_0	Q	A
z	b_0	b_0	b_1	b_0	b_1	b_0	Q	A
all	1	1	0	1	0	1	0	0

form allows us to compute the power spectrum derivatives in the Fisher matrix analytically. The Power Law bias model has the form [12]:

$$b(z, k) = b_0(z) + b_1(z) \left(\frac{k}{k_1} \right)^n, \quad (4)$$

where the pivot scale k_1 is introduced only to deal with dimensionless parameters. Its value does not impact our analysis and, without lack of generality, we set $k_1 = 1 h \text{ Mpc}^{-1}$. The slope n is not treated as a free parameter but is kept fixed. We note that the Power Law model is similar to the one proposed by [13] in those k -ranges in which the power spectrum can be approximated by a power law. The Q-Model is also phenomenological. It has been proposed by [6] from the analysis of mock halo and galaxy catalogs extracted from the Hubble volume simulation. Its analytical expression is:

$$b(z, k) = b_0(z) \left[\frac{1 + Q(z)(k/k_1)^2}{1 + A(z)(k/k_1)} \right]^{1/2}. \quad (5)$$

In our analysis all three parameters b_0 , Q and A are free to vary in each redshift bin. Therefore, the Q-Model has additional degrees of freedom with respect to the Power Law model. Finally, we need to specify the parameters of the fiducial model (denoted FM1-PL for the power law bias and FM1-Q for the Q-model). The parameters that identify the fiducial models are listed in Tab. 1. Note that we also consider for comparison the case of scale-independent bias (first row). This case is identical to choosing $n = 0$ in the power law model, i.e. to $b(z) = b_0(z) + b_1(z)$, so we will refer to this case as $n = 0$ fiducial. In order to evaluate the Fisher matrix we compute the derivatives of the power spectrum in Eq. (1) with respect to the parameters on the fiducial model. The 1σ error for each parameter of the model, p_i , is $\sigma_{p_i} = \sqrt{(F^{-1})_{ii}}$, where F^{-1} is the inverse Fisher matrix (for technical procedure see [5]).

3. Results

3.1. Power law case

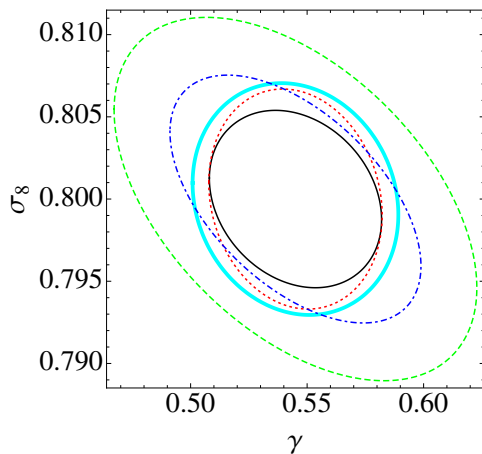
For the power law model we have explored two cases corresponding to different choices of the power law index: $n = 1$ and $n = 2$. The parameters of the fiducial models are reported in Tab. 1. The 1σ errors on the cosmological parameters are listed in Tab. 2. For all parameters except the mass variance σ_8 and the growth index γ the errors are largely independent from n . In fact, in most cases they slightly decrease when the scale dependence is stronger. The values of σ_8 and γ show the opposite trend, although the effect is quite small in respect to other parameters (below 10 %). We conclude that allowing for a scale dependent bias has little effect on the precision in which we can measure most cosmological parameters. It is interesting to note that the accuracy of the growth rate γ is 4-5% when marginalising over all parameters, including the scale and redshift-dependent bias.

The expected 1σ errors for the bias parameters b_0 and b_1 are listed in Tab. 3 for the cases $n = 0, 1, 2$: the errors on b_1 are larger than those on b_0 and their size increase with n , while when $n = 2$ they are ten times larger than $n = 1$. On the contrary, errors on b_0 weakly depend

Table 2. 1σ errors on cosmological parameters for the fiducial models adopted in this work (see [5]).

Error	$n = 0$	FM1-PL		FM1-Q
		$n = 1$	$n = 2$	
σ_h	0.036	0.038	0.037	0.039
$\sigma_{\Omega_m h^2}$	0.015	0.016	0.015	0.016
$\sigma_{\Omega_b h^2}$	0.0034	0.0036	0.0034	0.0036
σ_{n_s}	0.036	0.042	0.036	0.044
σ_γ	0.024	0.025	0.028	0.029
σ_{σ_8}	0.0036	0.0044	0.0045	0.0047

on n . This is not surprising since b_1 is constrained by the power spectrum behaviour at high k , the larger the value of n the larger the values of k , where our analysis is less sensitive due to the damping terms and the hard k_{max} cut. A second trend is with the redshifts: errors on the bias parameters increase with the redshift, irrespectively of the value of n as shown in Fig. 1. This merely reflects the fact that the effective volume of the survey monotonically decreases when moving to high redshifts due to the smaller galaxy densities.

**Figure 1.** 68 % probability contours for σ_8 and γ . Black, continuous: standard scale-independent case, i.e. $n = 0$. Red, Dotted: FM1-PL with $n = 1$. Cyan, continuous: FM1-Q. Blue, Dot-Dashed: FM2-PL with $n = 2$. Green, dashed: FM2-Q. The FM1-PL case when $n = 1$ is only slightly larger than that corresponding to a scale-independent bias (for further details see [5]).

When compared to the results of [12], in which bias was assumed to be scale-independent, we notice that our constraints on b_0 are twice weaker than their “optimistic, internal bias” case at $z = 1.8$ and $z = 2.0$. This quantifies the effect of allowing for an additional degree of freedom, the scale dependent bias, represented by the new parameter b_1 . In Fig. 2 we show the 68 % probability contours in the b_0 - b_1 plane for $n = 1$ and $n = 2$, respectively. Larger ellipses refer to higher redshift bins. For the case $n = 1$ there is a strong anti-correlation between b_0 and b_1 stemming from the fact that an increase in the linear bias term b_0 can be partially compensated by reducing the amplitude of the scale-dependent term b_1 . Increasing the scale dependency, i.e. setting $n = 2$ reduces the correlation between b_0 and b_1 . This is due to the fact that a strong scale dependent bias has little impact on large scales ($k \ll k_1$) and therefore cannot effectively compensate a variation of the linear bias on the scales that are relevant for our analysis.

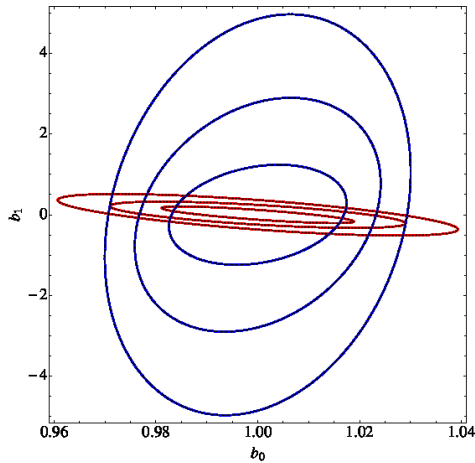
3.2. Q-model

This version of Type 1 fiducial model is characterised by three parameters, b_0 , A and Q , rather than two. We have repeated the same analysis performed as in the FM1-PL case and summarised

Table 3. Errors on bias parameters for the fiducial models adopted in this work (see [5]).

z	$n = 0$	FM1-PL				FM1-Q		
		$n = 1$		$n = 2$		σ_{b_0}	σ_Q	σ_A
	σ_{b_0}	σ_{b_0}	σ_{b_1}	σ_{b_0}	σ_{b_1}			
0.6	0.007	0.013	0.14	0.0081	1.2	0.017	3.04	0.35
0.8	0.008	0.013	0.13	0.0093	0.97	0.017	2.5	0.32
1.0	0.009	0.013	0.12	0.011	0.86	0.017	2.2	0.31
1.2	0.010	0.014	0.12	0.012	0.82	0.018	2.2	0.31
1.4	0.011	0.014	0.13	0.013	0.91	0.019	2.5	0.34
1.6	0.012	0.016	0.16	0.014	1.2	0.023	3.4	0.42
1.8	0.014	0.019	0.22	0.016	1.9	0.027	5.4	0.59
2.0	0.018	0.026	0.34	0.019	3.3	0.037	9.4	0.97

the results in Tabs. 2 and 3. The errors on the cosmological parameters are very similar to those obtained in the FM1-PL case, confirming that the accuracy in the estimate of the cosmological parameters is not much affected by the adoption of a scale-dependent bias model, even when we introduce an additional degree of freedom. Errors on the linear bias parameters b_0 (Tab. 3) are small, with a magnitude similar to that of the FM1-PL case with $n = 1$. On the contrary, the errors on A and Q are quite large, although we cannot directly compare their size to the errors on b_1 . This is not entirely surprising: it is the effect of having one more parameter to marginalize over. To further investigate the possible degeneracy among the bias parameters we plot the 68 % uncertainty contours in the A - Q plane in Fig. 3. The size of the errors, and consequently the area of the corresponding ellipse increases with the redshift. They are positively correlated and the strength of the correlation also increases with the redshift.

**Figure 2.** 68% probability contours for the parameters b_0 and b_1 of the FM1-PL model. The dotted red line is the case with $n = 1$ while the dashed line in blue shows the case $n = 2$. The redshift bins are $z = 0.6, 1.8, 2.0$ (see [5]).

4. Conclusions

We have investigated the impact of a scale-dependent galaxy bias on the results of the clustering analysis performed in next generation surveys (see [5]). Our main results can be summarised as follows:

- Allowing for a scale dependent bias does not increase significantly the errors on cosmological parameters, except for the growth index γ and the rms density fluctuation σ_8 . More specifically, in our analysis we find that errors on h_0 , Ω_{m0} , Ω_{b0} , Ω_{k0} , and n_s are only

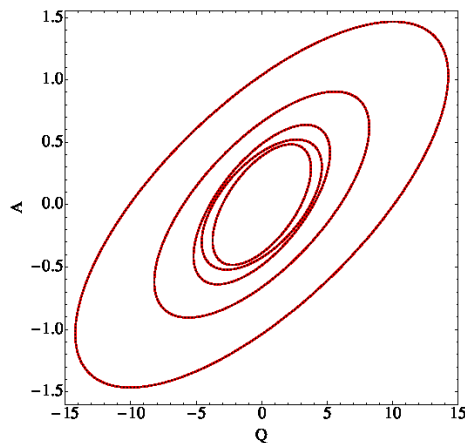


Figure 3. 68 % probability contours for the parameters A and Q of the FM1-Q model. We decided to plot only the bins $z = 0.6, 0.8, 1.6, 1.8, 2.0$, to improve clarity: larger values of redshift correspond to ellipses with larger semiaxis.

slightly larger than those expected when one assumes that bias is scale independent. In addition, γ and σ_8 are correlated. This correlation is expected since the clustering analysis constrains the amplitude of the power spectrum, proportional to the product $b(k, z)\sigma_8(z)$ and its redshift distortions, which are proportional to $f(z)/b(k, z)$.

- The linear bias parameter b_0 can be determined within a few %. The relative error is rather insensitive to the choice of the fiducial and slightly increases with the redshift. As expected, the errors increase with the number of free parameters in the model and therefore is larger in the Q-Model than in the Power Law one.
- The accuracy with which one can estimate the bias parameters that describe the scale dependency depends on the bias model and on the fiducial model. This is not surprising since in this case the scale dependence is pushed at small scales, where our Fisher matrix analysis, optimised to probe linear to mildly nonlinear scales, is less sensitive.

Acknowledgments

The research leading to these results has received funding from the European Research Council under the European Community Seventh Framework Programme (*FP7/2007 – 2013 Grant Agreement no. 279954*), therefore the financial support provided by Della Riccia Fellowship. EM acknowledges L. Amendola, M. Corsi, C. Di Porto and E. Branchini.

References

- [1] Seo H J and Eisenstein D J 2007 *Astrophys. J.* **665** 14.
- [2] Comparat J *et al.* 2013 *MNRAS* **433** 1146.
- [3] Schlegel D, Abdalla F, Abraham T, Ahn C, Allende Prieto C, Annis J, Aubourg E and Azzaro M 2011 arXiv:1106.1706.
- [4] Di Porto C, Amendola L and Branchini E 2012 *MNRAS* **423** L97-L101.
- [5] Amendola L, Menegoni E, Di Porto C, Corsi M and Branchini E 2015 Accepted by *Phys. Rev. D* arXiv:1502.03994v1.
- [6] Cole S *et al.* 2005 *MNRAS* **362** 505.
- [7] The catalogs are publicly available at <http://astro.dur.ac.uk/d40qra/lightcones/EUCLID/>.
- [8] Laureijs R. *et al.* 2011 arXiv:1110.3193.
- [9] Seo H J and Eisenstein D J 2003 *Astrophys. J.* **598** 720.
- [10] Seljak U 2001 *MNRAS* **325** 1359.
- [11] Tegmark M 1997 *Phys. Rev. Lett.* **79** 3806.
- [12] Di Porto C, Amendola L and Branchini E 2012 *MNRAS* **419** 985 1101.2453.
- [13] Seo H.J and Eisenstein D. J. 2005 *Astrophys. J.* **633** 575.